

Porous Co₃O₄ Nanoflakes as Anode Material for Lithium Ion Batteries

Yu Yao, Jingjing Zhang, Tao Huang*, Han Mao, Aishui Yu*

Department of Chemistry, Shanghai Key Laboratory of Molecular Catalysis and Innovative Materials, Institute of New Energy, Fudan University, Shanghai 200438, China

*E-mail: asyu@fudan.edu.cn; huangt@fudan.edu.cn

Received: 27 December 2012 / Accepted: 22 February 2013 / Published: 1 March 2013

A simple approach to mass produce Co₃O₄ using urea (CON₂H₄) as a precipitate via hydrothermal treatment has been developed. The samples were calcined at different temperatures and tested as an anode material for lithium ion battery. Scanning electron microscopy (SEM) images of the Co₃O₄ prepared at 600 °C showed a porous nanoflake morphology. The material is flaky with nanopores on the surface planes, forming a two-dimensional network structure. The electrochemical measurements showed that the porous Co₃O₄ nanoflakes had good electrochemical performance with a capacity of 824 mAh g⁻¹ after the 50th cycle at a current density of 100 mA g⁻¹. The excellent electrochemical properties could be attributed to its unique two-dimensional network structure.

Keywords: Co₃O₄; Porous nanoflake; Anode material; Lithium ion battery

1. INTRODUCTION

Lithium-ion batteries with long cycle life and high energy density are regarded as promising power sources for electric devices and portable electronics [1-3]. Currently, commercial lithium ion batteries use graphite as anode material; however, the low capacity of graphite cannot meet the increasing energy demand of modern devices. In recent years, research efforts have been undertaken to develop new anode materials to replace carbon and improve the energy density of lithium ion batteries. It has been proposed that transition metal oxides, MO(M: Co, Ni, Cu, Fe), could be used as new anode materials due to their high lithium storage capacity [4].

Among the transition metal oxides, Co₃O₄ has attracted a great deal of attention because of its high theoretical capacity (890 mAh g⁻¹) [5, 6]. However, Co₃O₄ suffers from poor capacity retention and rate capacity, which has been attributed to the large volume changes during cycling. It is well known that the morphology and microstructure of Co₃O₄ greatly influence the properties, and thus, a

variety of Co_3O_4 nanostructures have been synthesized. These reported Co_3O_4 nanostructured materials have better lithium ion storage properties than their bulk counterparts, and include but are not limited to nanotubes [7,8], nanorods [13], nanoneedles [11,12], platelets [14], nanowires [9,10] and nanospheres [15].

In this study, we report on a simple hydrothermal treatment to obtain Co_3O_4 nanoflakes. The synthesis initially involved the formation of a precursor by a chemical bath deposition method, from which nanoflakes were obtained from subsequent hydrothermal and heat treatments. The morphology and electrochemical properties of the prepared Co_3O_4 materials were investigated in detail.

2. EXPERIMENTAL

2.1 Preparation of porous Co_3O_4 nanoflakes

In a typical synthesis, 0.87 g $\text{Co}(\text{NO}_3)_2 \cdot 6\text{H}_2\text{O}$, 0.6 g urea and 0.4 g PEG-2000 were dissolved in 40 ml deionized water. The solution was then put into a 50 ml Teflon-lined stainless steel autoclave and maintained at 85 °C for 8 h. The autoclave was then heated to 200 °C and held at that temperature for 16 h. After cooling to room temperature, the precipitate was collected and washed several times with deionized water and alcohol. This precipitate was dried at 70 °C, and subsequently annealed in a Muffle furnace for 3 h. After being cooled to room temperature, Co_3O_4 materials with different morphologies were obtained.

2.2 Characterization

The morphology of the as-prepared Co_3O_4 materials was observed by scanning electron microscopy (SEM, JEOL JSM-6390). X-ray diffraction (XRD) was performed on a Brüker D8 Advance and Davinci Design X-ray diffractometer using $\text{Cu K}\alpha$ radiation with a wavelength of 1.5406 Å and a scan rate of 4° min^{-1} within the range of 10 to 90°.

2.3 Electrochemical measurement

The electrochemical performance of the prepared Co_3O_4 materials was evaluated using coin cells assembled in an argon-filled glove box (Mikarouna, Superstar 1220/750/900). An assembled coin cell was composed of lithium as the counter/reference electrode and the working electrode prepared pasting the active material, super P carbon black and polyvinylidene fluoride (PVDF) with a weight ratio of 80:10:10, using 1-methyl-2-pyrrolidinone (NMP) as solvent onto copper foil. The resulting film was dried at 80°C in a vacuum for 12 h to evaporate the NMP. The electrolyte solution used was 1 M LiPF_6 dissolved in ethylene carbonate (EC) and dimethyl carbonate (DEC) (1:1 in volume) and a microporous polypropylene film (Celgard 2300) was used as separator. The electrochemical performance of the prepared materials was tested by cyclic voltammetry, galvanostatically charging and discharging tests. Cyclic voltammetry was carried out in the potential range from 3 V to 0 V (vs.

Li/Li⁺), at a scan rate of 0.2 mV s⁻¹ on an electrochemical workstation (CH Instrument 660C, CHI Company). The galvanostatic charge–discharge tests were performed on a battery test system (Land CT2001A, Wuhan Jinnuo Electronic Co. Ltd.) at a constant current density of 100 mA g⁻¹ in the potential range from 0.01 to 3.0 V.

3. RESULT AND DISCUSSION

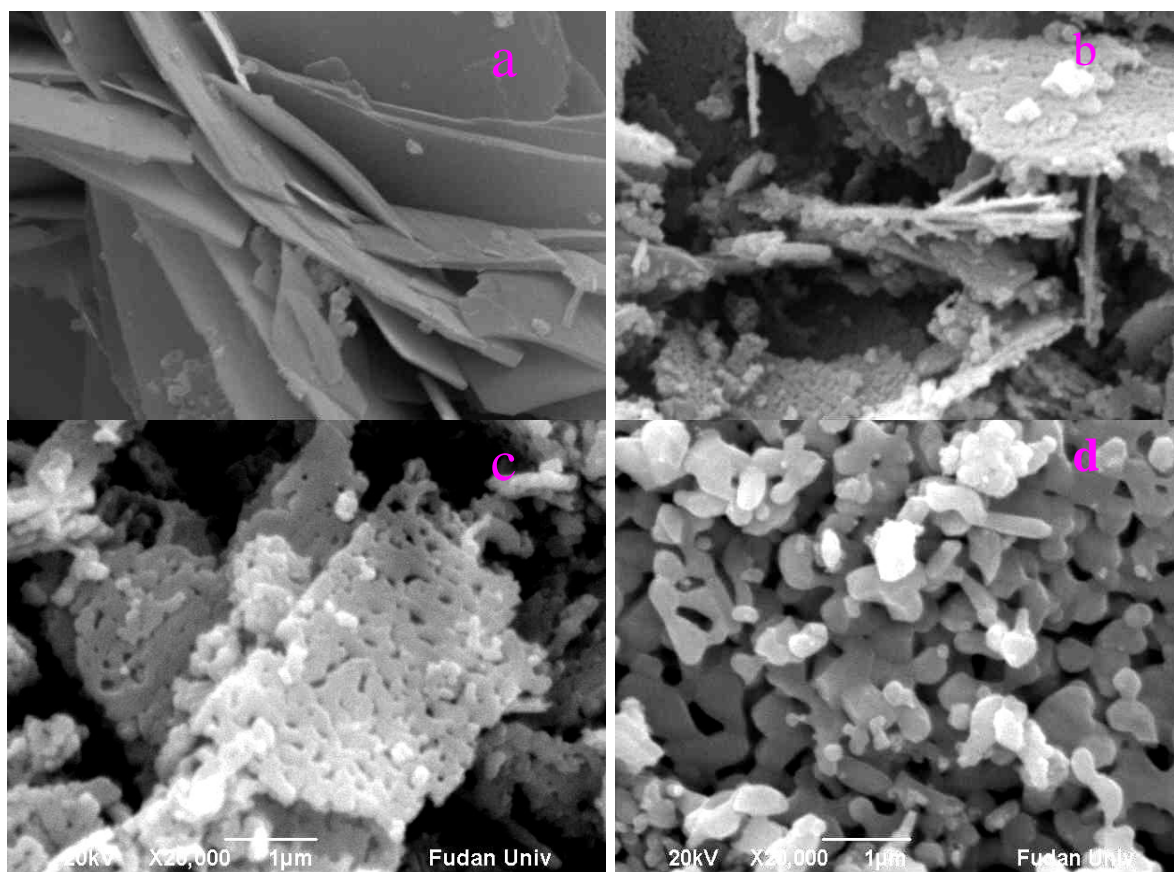


Figure 1. SEM images of the precursor obtained at 200 °C (a), and the Co₃O₄ materials prepared by calcinating the flake-like precursor at 500 °C (b), 600 °C (c) and 700 °C (d).

Fig. 1a shows an SEM image of the precursor obtained at 200 °C by hydrothermal treatment. The image clearly shows that the precursor exhibits a flakey structure which is formed with assistance of PEG. The uniform and ordered chain structure of PEG is easily adsorbed at the surface of the metal oxide colloid. The growth rate of the colloids in specific directions will be confined when the surface of the colloid adsorbs the PEG molecule, leading to anisotropic growth of the crystals. The hydrothermal product adopted a flake-like morphology due to the incorporation of PEG. Fig. 1b, Fig. 1c and Fig. 1d display the SEM images of Co₃O₄ prepared by calcinating the flake-like precursor at 500

°C, 600 °C and 700 °C, respectively. It can be observed that the Co_3O_4 material prepared at 500 °C has concave indentations on the surface. When the temperature was raised to 600 °C, many pores appear on the surface of Co_3O_4 nanoflakes that form a two-dimensional network. However, the Co_3O_4 material prepared at 700 °C does not exhibit the flake-like structure, but rather fragments into small pieces. The nanopores on the Co_3O_4 material prepared at 600 °C might be generated through the decomposition of the precursor and the release of water and carbon dioxide, which can induce a different morphology of the as-prepared material at different temperatures. From these SEM images, it is revealed that the optimal annealing temperature for the formation of porous Co_3O_4 nanoflakes is 600 °C.

The crystal structures of prepared Co_3O_4 materials calcined at 500 °C, 600 °C and 700 °C were characterized by XRD, the corresponding patterns of which are exhibited in Fig. 2.

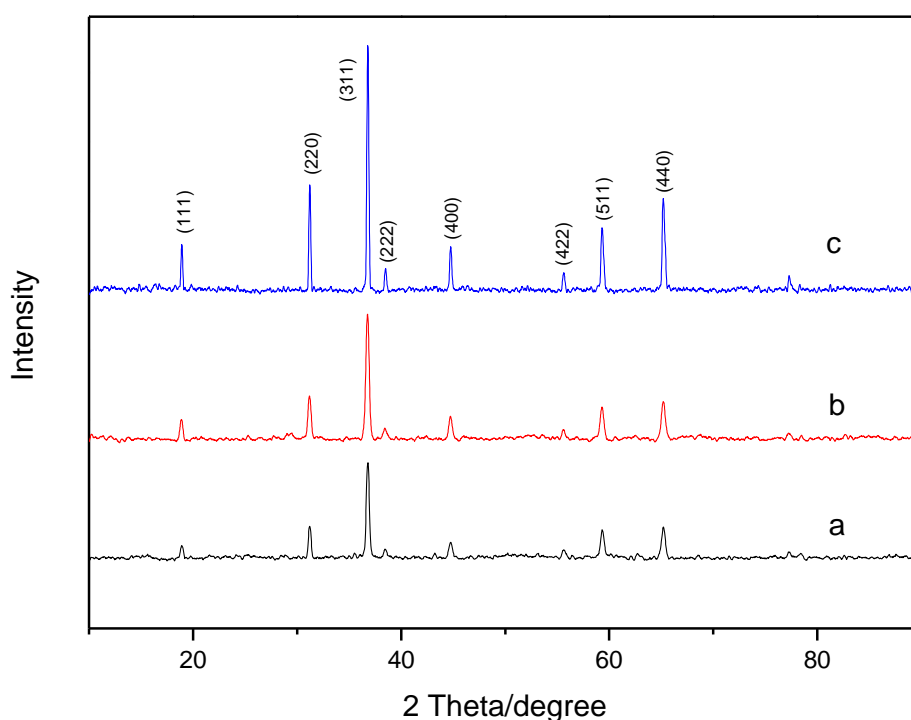


Figure 2. XRD pattern of the Co_3O_4 materials prepared by calcinating the flake-like precursor at 500 °C (a), 600 °C (b) and 700 °C (c).

All the reflections can be indexed to the typical Co_3O_4 phase with lattice constant $a = 8.084 \text{ \AA}$ (space group $Fd3m$ [227]), and corresponding to the standard crystallographic data (PDF card No.43-1003). No secondary or impurity phases were detected, indicating high purity of the final products. The main peaks at 19.0° , 31.3° , 36.8° , 44.8° , 59.4° and 65.2° can be assigned to the (111), (220), (311), (400), (511) and (440) reflections of Co_3O_4 , respectively. When the calcination temperature was increased from 500 to 700 °C, the XRD peaks gradually became sharper and more intense, indicating an increase in crystallinity potentially due to grain growth, ordering of local structure and release of the lattice strain. The crystallite size of the Co_3O_4 materials is estimated by the Scherrer equation, and the average size of the crystallite is calculated to be approximately 26, 29 and 44 nm corresponding to materials prepared at 500, 600 and 700 °C, respectively.

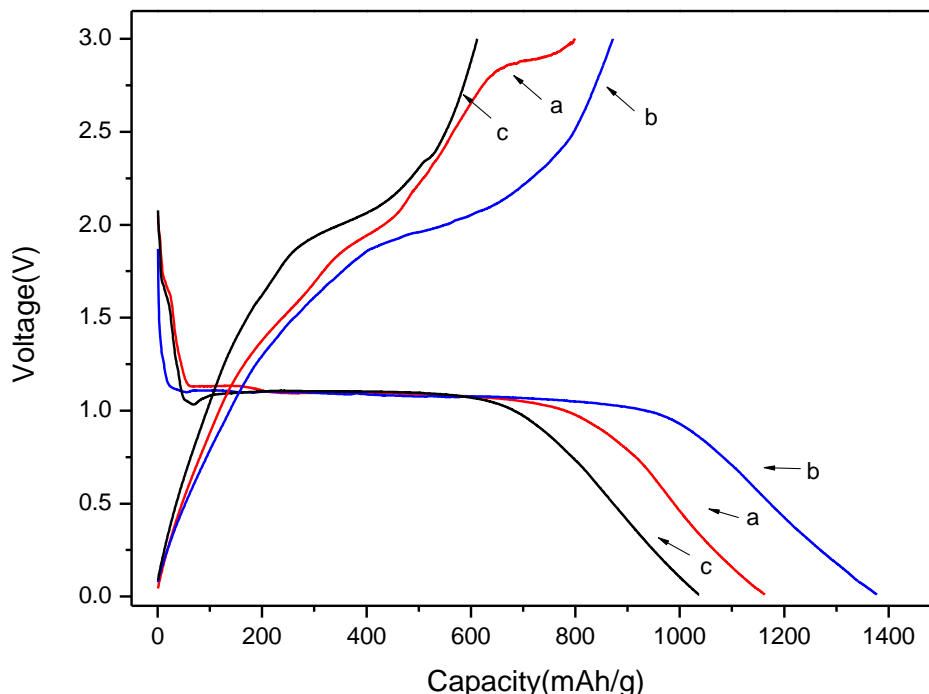


Figure 3. The first discharge and charge curves of the Co_3O_4 materials prepared by calcinating the flake-like precursor at 500 °C (a), 600 °C (b) and 700 °C (c).

Fig. 3 displays the initial discharge and charge curves of the Co_3O_4 electrodes prepared at different temperature. The discharge curves are qualitatively very similar, indicating the same electrochemical behavior. The initial discharge curve shows a clear potential plateau at approximately 1.1 V vs Li^+/Li , and the following sloping region may be attributed to the formation of a solid electrolyte interphase (SEI) film which can cause irreversible capacity loss. The first discharge capacities of Co_3O_4 electrodes prepared at 500, 600 and 700 °C are 1163, 1377 and 1037 mAh g^{-1} , respectively, which are all larger than the theoretical value (890 mAh g^{-1}). This phenomenon has been widely reported for transition metal oxides and is typically ascribed to irreversible reactions that form the SEI film and possibly result in interfacial lithium storage. The charging curves trends are also similar, and the capacities are 800, 871, and 611 mAh g^{-1} . The initial Coulombic efficiencies can be calculated as 68.8%, 63.3% and 59.0%.

The cyclic voltammetry measurements were performed to test the electrochemical properties of the porous Co_3O_4 nanoflake electrode during the galvanostatic charge-discharge process. Fig. 4 exhibits the first three complete cycles performed at a sweep rate of 0.2 mV s^{-1} from 0 to 3 V. In the first reduction process, a strong reduction peak at 0.8 V is observed, corresponding to the initial reduction of Co_3O_4 to metallic Co ($\text{Co}_3\text{O}_4 + 8\text{Li}^+ + 8\text{e}^- \rightarrow 3\text{Co} + 4\text{Li}_2\text{O}$) and the growth of the gel-like SEI layer which contains ethylene-oxide-based oligomers, LiF, Li_2CO_3 and lithium alkyl carbonate (ROCO_2Li)[16]. In the first oxidation process, there is a peak at 2.04 V, corresponding to the reaction $3\text{Co} + 4\text{Li}_2\text{O} \rightarrow \text{Co}_3\text{O}_4 + 8\text{Li}^+ + 8\text{e}^-$. The reduction peaks in the subsequent second and third cycles are weaker than first cycle after the electrode was activated during the first cycle, and the oxidation peaks tend to be overlapping.

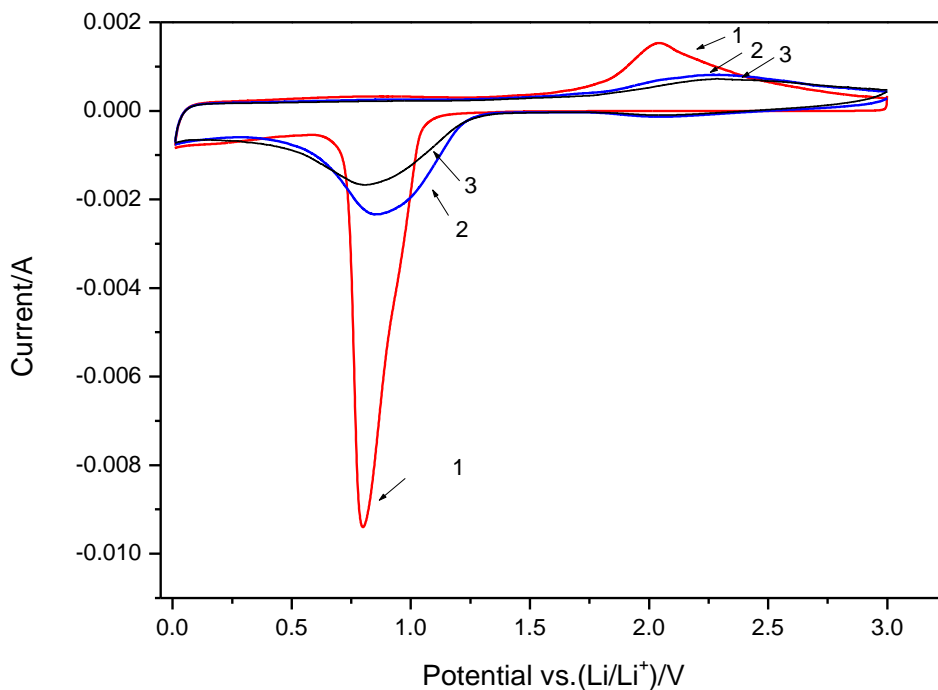


Figure 4. Cyclic Voltammograms of the Co_3O_4 electrode materials prepared by calcinating the flake-like precursor at $600\text{ }^\circ\text{C}$ measured between 0 and 3V at the scan rate of 0.2 mV s^{-1} .

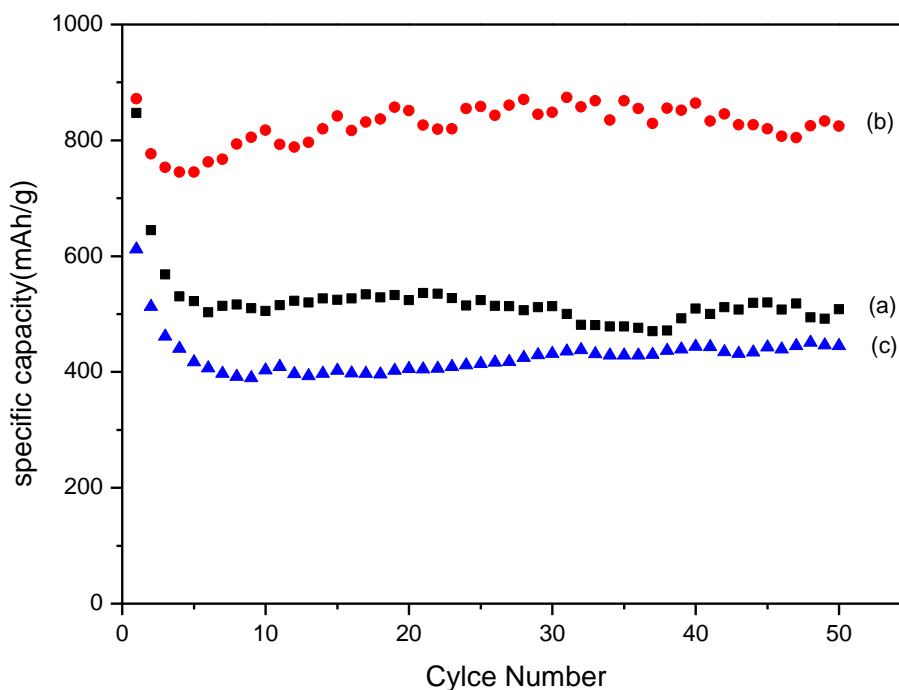


Figure 5. Cycling performance of the Co_3O_4 materials prepared by calcinating the flake-like precursor at $500\text{ }^\circ\text{C}$ (a), $600\text{ }^\circ\text{C}$ (b) and $700\text{ }^\circ\text{C}$ (c) at the current density of 100 mA g^{-1} .

Fig. 5 shows the cycling performance of the three electrodes at a current density of 100 mA g^{-1} . It is found that the Co_3O_4 electrode prepared at $600\text{ }^\circ\text{C}$ demonstrates the best cycling performance and

delivers an initial discharge capacity of 872 mAh g^{-1} and remains at 824 mAh g^{-1} following the 50th cycle. The Co_3O_4 electrodes prepared at 500 and 700 °C exhibit discharge capacity of 508 and 445 mAh g^{-1} after the 50th cycle, respectively. The strong electrochemical performance of the Co_3O_4 electrode prepared at 600 °C can be attributed to its novel nanostructure composed of porous nanoflakes. The flakey morphology and the pores on the flakes form a net-like structure which allows enhances electrolyte penetration, leading to large contact interfaces between the electrode and electrolyte and short diffusion paths for lithium ions. The porous structure can also better accommodate the volume changes experienced during cycling, and alleviate pulverization of the active electrode material. These aspects lead to the improvements of the electrochemical properties. The high rate electrochemical performance of the Co_3O_4 electrode prepared at 600 °C was investigated using the multiple-step galvanostatic strategy, and the results are shown in Fig. 6.

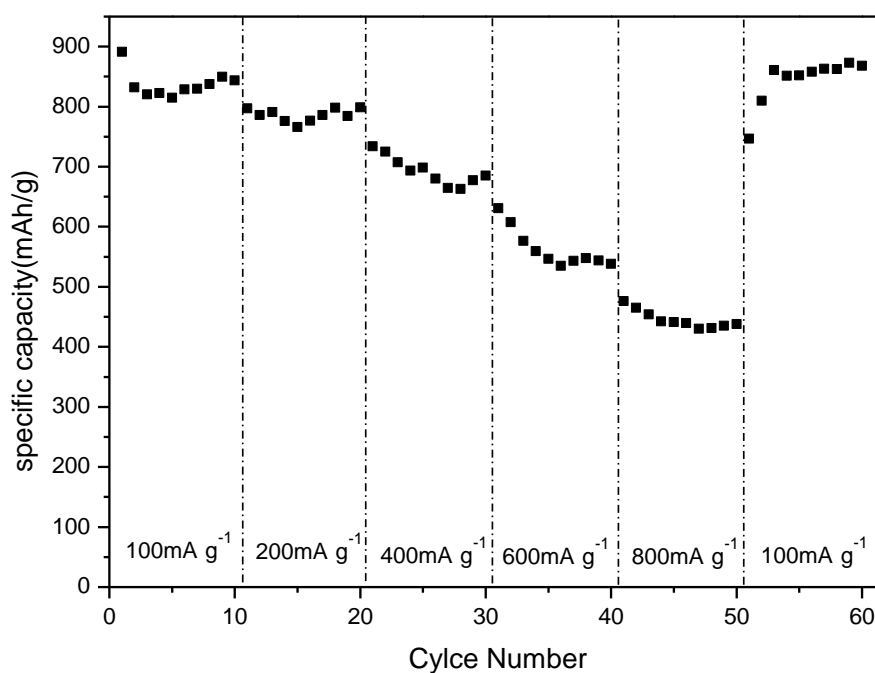


Figure 6. The electrochemical performance of the Co_3O_4 materials prepared by calcinating the flake-like precursor at 600 °C by multiple step galvanostatic testing (at the current density of 100, 200, 400, 600, 800 mA g^{-1} and then return to the 100 mA g^{-1} step by step).

For each step, 10 cycles were measured to evaluate the rate performance. The average discharge capacities of the Co_3O_4 at 100, 200, 400, 600 and 800 mA g^{-1} were 842, 785, 707, 546 and 454 mAh g^{-1} , respectively, much higher than that of commercial graphite. The capacity then returned to 851 mAh g^{-1} when the current density was restored to 100 mA g^{-1} , suggesting that the porous Co_3O_4 nanoflake morphology supports high-rate charge/discharge capacities.

4. CONCLUSIONS

We developed a novel approach to prepare porous Co_3O_4 nanoflakes as anode material for lithium ion batteries. The porous Co_3O_4 nanoflakes have been synthesized by a simple hydrothermal method using urea (CON_2H_4) as a precipitate combined with hydrothermal treatment and calcination at $600\text{ }^\circ\text{C}$. The as-prepared Co_3O_4 material exhibits a nanoflake morphology, and there are nanopores on the individual flakes, which results in a two-dimensional net-like structure. Electrochemical measurements indicated that the porous Co_3O_4 nanoflakes had excellent electrochemical performance with a capacity of 824 mAh g^{-1} after the 50th cycle at a current density of 100 mA g^{-1} . The strong electrochemical performance of the porous Co_3O_4 nanoflakes can be attributed to the two-dimensional net-like structure that offers good electronic contact of the active material with the electrolyte, short pathways for lithium ion diffusion, and increased tolerance of any volume changes.

ACKNOWLEDGEMENTS

The authors acknowledge funding support from “973” Program (No. 2013CB934103), the National Natural Science Foundation (No. 21173054) and Science & Technology Commission of Shanghai Municipality (No. 08DZ2270500), China.

References

1. B. Scrosati, *Nature* 373 (1995) 557-558.
2. J. Y. Luo, H.M. Xiong and Y.Y. Xia, *J. Phys. Chem. C* 112 (2008) 12051-12057.
3. R.F. Nelson, *J. Power Sources* 91 (2000) 2-26.
4. P. Poizot, S. Laruelle, S. Grugeon, L. Dupont, J.M. Tarascon, *Nature* 407 (2000) 496-499.
5. X. Wang, L.J. Yu, X.L. Wu, F.L. Yuan, Y.G. Gao, Y. Ma, J.N. Yao, *J. Phys. Chem. C* 113 (2009) 15553-15558.
6. B. Guo, C.S. Li, Z.Y. Yuan, *J. Phys. Chem. C* 114 (2010) 12805-12817.
7. W.Y. Li, L.N. Xu, J. Chen, *Adv. Funct. Mater.* 15 (2005) 851-857.
8. N. Du, H. Zhang, B. Chen, J. Wu, X. Ma, Z. Liu, Y. Zhang, D. Yang, X. Huang, J. Tu, *Adv. Mater.* 19 (2007) 4505-4509.
9. H. Zhang, J. Wu, C. Zhai, X. Ma, N. Du, J. Tu, D. Yang, *Nanotechnology* 19 (2008) 035711
10. X.W. Lou, D. Deng, J.Y. Lee, J. Feng, L.A. Archer, *Adv. Mater.* 20 (2008) 258-262.
11. X.W. Lou, D. Deng, J.Y. Lee, L.A. Archer, *J. Mater. Chem.* 18 (2008) 4397-4401.
12. W. Yao, J. Yang, J. Wang, Y. Nuli, *J. Electrochem. Soc.* 155 (2008) A903-A908.
13. K.T. Nam, D.W. Kim, P.J. Yoo, C.Y. Chiang, N. Meethong, P.T. Hammond, Y.M. Chiang, A.M. Belcher, *Science* 312 (2006) 885-888.
14. Y. Li, B. Tan, Y. Wu, *Nano Lett.* 8 (2008) 265-270.
15. Y. liu, C. Mi, L. Su, X. Zhang, *Electrochim. Acta* 53 (2008) 2507-2513.
16. G. Gachot, S. Grugeon, M. Armand, S. Pilard, P. Guenet, J.M. Tarascon, S. Laruelle, *J. Power Sources* 178 (2008) 409-421.